The Astronomical Journal, 126:53–62, 2003 July

PECULIAR BROAD ABSORPTION LINE QUASARS FOUND IN THE DIGITIZED PALOMAR OBSERVATORY SKY SURVEY[1]

Robert J. Brunner[2]
Palomar Observatory, MS 105-24, California Institute of Technology, Pasadena, CA 91125; rb@astro.caltech.edu

Patrick B. Hall
Departamento de Astronomía y Astrofísica, Facultad de Física, Pontificia Universidad Católica de Chile, Casilla 306, Santiago 22, Chile; and Princeton University Observatory, Peyton Hall, Princeton, NJ 08544-1001

S. George Djorgovski, R. R. Gal,[3] A. A. Mahabal, P. A. A. Lopes, R. R. de Carvalho,[4] S. C. Odewahn,[5] S. Castro,[6] and D. Thompson
Palomar Observatory, MS 105-24, California Institute of Technology, Pasadena, CA 91125

F. Chaffee
W. M. Keck Observatory, 65-1120 Mamalahoa Highway, Kamuela, HI 96743

and

J. Darling[7] and V. Desai[8]
Palomar Observatory, MS 105-24, California Institute of Technology, Pasadena, CA 91125
Received 2003 March 25; accepted 2003 April 9

ABSTRACT

With the recent release of large (i.e., $\gtrsim$100 million objects), well-calibrated photometric surveys, such as Digitized Palomar Observatory Sky Survey (DPOSS), Two Micron All Sky Survey, and Sloan Digital Sky Survey, spectroscopic identification of important targets is no longer a simple issue. In order to enhance the returns from a spectroscopic survey, candidate sources are often preferentially selected to be of interest, such as brown dwarfs or high-redshift quasars. This approach, while useful for targeted projects, risks missing new or unusual species. We have, as a result, taken the alternative path of spectroscopically identifying interesting sources with the sole criterion being that they are in low-density areas of the $g-r$ and $r-i$ color space defined by DPOSS. In this paper, we present three peculiar broad absorption line quasars that were discovered during this spectroscopic survey, demonstrating the efficacy of this approach. PSS J0052+2405 is an iron low-ionization broad absorption line (LoBAL) quasar at a redshift $z = 2.4512 \pm 0.0001$ with very broad absorption from many species. PSS J0141+3334 is a reddened LoBAL quasar at $z = 3.005 \pm 0.005$ with no obvious emission lines. PSS J1537+1227 is an iron LoBAL at a redshift of $z = 1.212 \pm 0.007$ with strong narrow Mg II and Fe II emission. Follow-up high-resolution spectroscopy of these three quasars promises to improve our understanding of BAL quasars. The sensitivity of particular parameter spaces, in this case a two-color space, to the redshift of these three sources is dramatic, raising questions about traditional techniques of defining quasar populations for statistical analysis.

Key words: quasars: absorption lines — quasars: emission lines — quasars: general — surveys

1. INTRODUCTION

Quasars have been studied for 40 years now (e.g., Sandage 1965), but our understanding of them is still sketchy in many ways. The currently accepted paradigm is that quasars derive their luminosity from accretion onto supermassive black holes (see, e.g., Small & Blandford 1992). However, the detailed structure of the central engine is a mystery: we do not know exactly how matter accretes onto the black hole, although an accretion disk seems likely; we do not know why some quasars have strong jets (or how they are formed); and we do not know exactly how broad absorption line (BAL) outflows fit into the overall quasar model, even though the mass-loss rates in such outflows could be comparable to the overall accretion rates (e.g., Scoville & Norman 1995).

BAL quasars show absorption from gas with blueshifted outflow velocities of typically $0.1c$ (for a good overview of BAL quasars, see Weymann 1995). Most known BAL quasars are "HiBALs," with absorption only from high-ionization species like C IV, but about 15% are "LoBALs," which also show absorption from low-ionization species like

[1] Some of the data presented herein were obtained at the W. M. Keck Observatory, which is operated as a scientific partnership among the California Institute of Technology, the University of California, and the National Aeronautics and Space Administration. The Observatory was made possible by the generous financial support of the W. M. Keck Foundation.

[2] Current address: Department of Astronomy, University of Illinois, 1002 West Green Street, Urbana, IL 61801.

[3] Current address: Department of Physics and Astronomy, Johns Hopkins University, 3400 North Charles Street, Baltimore, MD 21218.

[4] Current address: Observatório Nacional, Rua General José Cristino 77, 20921-400 Rio de Janeiro, RJ, Brazil.

[5] Current address: Department of Physics and Astronomy, Arizona State University, P.O. Box 871504, Tempe, AZ 85287.

[6] Current address: Infrared Processing and Analysis Center, 770 South Wilson Avenue, Pasadena, CA 91125.

[7] Current address: Department of Astronomy, Cornell University, Ithaca, NY 14853.

[8] Current address: Department of Astronomy, University of Washington, Box 351580, Seattle, WA 98195.

Mg II. The rare iron LoBALs, or FeLoBALs, also show absorption from excited fine-structure levels or excited atomic terms of Fe II or Fe III.

Recent spectroscopic surveys for quasars, such as the 2dF QSO Redshift Survey (Boyle et al. 1999) and the Sloan Digital Sky Survey (SDSS; Schneider et al. 2002), have dramatically increased the number of spectroscopically confirmed quasars. As a direct result, the number of known BALs, and in particular, LoBALs and FeLoBALs, has increased as well, enabling the identification of peculiar quasars, whose BAL outflows show properties never before seen. Due to their peculiar nature, detailed studies of these quasars often provide important insight into the physical characteristics of BAL outflows and quasar models in general. Before high-resolution spectroscopy can be employed on these systems, however, these peculiar quasars must be found.

Due to their rare nature, identifying candidates of such objects requires large photometric surveys, such as the FIRST radio survey (Becker et al. 1997), the SDSS (York et al. 2000), and the Digitized Palomar Observatory Sky Survey (DPOSS; Djorgovski et al. 2001). From the catalogs that are generated from these surveys, different selection criteria have been employed to pick suitable candidates for spectroscopic follow-up.

In this paper, we present three peculiar BAL quasars that were discovered during a spectroscopic follow-up of color-space outliers from the DPOSS. We outline the observations used in § 2, analyze the spectra in § 3, and discuss some implications of these objects and summarize our conclusions in § 4.

2. OBSERVATIONS

The quasars presented in this paper were initially targeted because of their location in the $g-r$ and $r-i$ color space as quantified by DPOSS. DPOSS is detailed extensively elsewhere (Djorgovski et al. 2001, and references therein). In order to clarify the selection of these three sources, however, the rest of this section provides a brief overview of DPOSS.

DPOSS is based on the POSS-II photographic survey (Reid et al. 1991), which covers the northern sky ($\delta > -3^\circ$). The POSS-II plates were obtained at the 48 inch (1.2 m) Oschin Schmidt telescope at Palomar in three bands: blue-green, IIIa-J + GC 395; red, IIIa-F + RG 610; and near-IR, IV-N + RG 9. The plates were obtained following a strategy based on 897 fields, where each field is approximately $6\overset{\circ}{.}5$ on a side (i.e., the size of an individual plate), while the individual field centers are spaced 5° apart. As a result, nearly half of the total survey area is covered by more than one plate, improving the overall calibration.

The photographic plates were digitized using a modified PDS scanner at STScI (Lasker et al. 1996) producing a digital image that is 23,040 pixels square, with $1''$ pixels. Each image file is approximately one gigabyte in size, and the total survey is nearly three terabytes. The digital image files for all scans $\delta > 15^\circ$ were processed using the SKICAT software (Weir et al. 1995), producing a catalog of approximately 60 parameters for each object. Object classification was performed using a subset of these parameters as described in Odewahn et al. (2003).

The photographic catalog data was calibrated using CCD calibration data in the g, r, and i filters (Gal et al. 2003). A second correction was applied to the catalog to correct for plate vignetting (Mahabal et al. 2003). Finally, extinction corrections were applied using the Schlegel, Finkbeiner, & Davis (1998) prescription. The typical limiting magnitudes for the calibrated catalog data are $g_J \sim 20.5$ mag, $r_F \sim 20.7$ mag, and $i_N \sim 20.3$ mag. The three sources presented in this paper are shown in Figure 1, along with random stellar sources with similar magnitudes to the quasars presented herein. In addition, the coordinates, magnitudes, and measured redshifts for these sources are provided in Table 1.

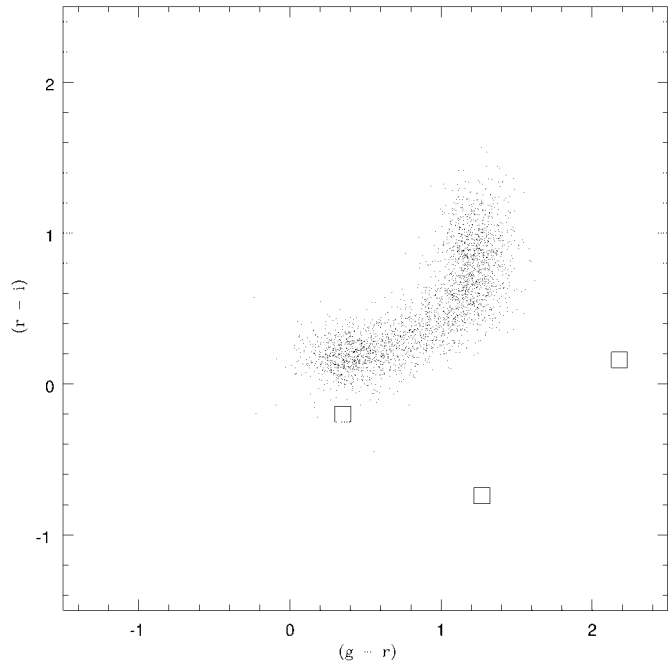

FIG. 1.—Color space used to select color outliers. The three quasars presented in this paper are marked by the large squares. The small dots are several thousand stellar sources, with similar magnitudes to the quasars presented herein, extracted randomly from the survey.

2.1. *Optical Spectroscopy*

Discovery spectra of all three objects were obtained at the Palomar Observatory 200 inch (5 m) Hale telescope, using the Double Spectrograph (DBSP) instrument (Oke & Gunn 1982). All observations used a $2''$ wide, long slit, and in all cases the slit position angle was close to the parallactic. Exposures of standard stars from Oke & Gunn (1983) were used to remove the instrument response function and provide at least a rough flux calibration, and exposures of arc lamps were used to derive the wavelength solutions. All data were processed using standard techniques.

Observations of PSS J0052+2405 (see Fig. 2) were made on 1997 September 2 and 4 UT, in nonphotometric conditions. A set of exposures with integration times of 200, 400, and 1200 s were obtained. We used a 300 lines mm^{-1} grating on the blue side of the DBSP, giving a dispersion of 2.17 Å $pixel^{-1}$ and a FWHM resolution of 11 Å, covering the wavelength range from ~3360 to 6860 Å. On the red side, we used a 316 lines mm^{-1} grating giving a dispersion of 3.06 Å $pixel^{-1}$ and a resolution of 11 Å, covering the wavelength range ~6760–9290 Å. A dichroic with a split wavelength near 6800 Å was used.

Observations of PSS J0141+3334 (see Fig. 3) were obtained on 1999 November 10 UT, in good conditions; exposure times were 120 and 800 s. We used gratings with

TABLE 1
COORDINATES, MAGNITUDES, AND REDSHIFTS FOR THE THREE PECULIAR BAL QUASARS PRESENTED IN THIS PAPER

Source Name	R.A. (J2000.0)	Decl. (J2000.0)	g	r	i	Redshift
PSS J0052+2405[a]	00 52 06.8	+24 05 39	19.37	18.08	18.87	2.45
PSS J0141+3334[b]	01 41 32.9	+33 34 24	20.88	18.70	18.54	3.01
PSS J1537+1227[a]	15 37 41.8	+12 27 44	18.67	18.26	18.52	1.21

NOTE.—Units of right ascension are hours, minutes, and seconds, and units of declination are degrees, arcminutes, and arcseconds.

[a] The data for these quasars are publicly available from the DPOSS science archive (see http://www.dposs.caltech.edu/).

[b] The magnitudes for this quasar are approximate, since this source does not lie within the well-calibrated area that has been released to the public.

600 lines mm^{-1} (blue) and 158 lines mm^{-1} (red), covering the wavelength ranges ~3400–5200 Å (blue) and ~5120–10100 Å (red), and a 5200 Å dichroic. This is the discovery spectrum shown in Figure 4 and used in the analysis presented in this paper.

Observations of PSS J1537+1227 (see Fig. 5) were obtained on 1996 May 21 UT, in mediocre conditions, with exposures of 300 and 900 s. The same gratings were used, but with a 5500 Å dichroic, and the wavelength coverage was ~3900–5600 Å (blue side) and ~5550–8070 Å (red side). Additional data were obtained on 1999 May 12 UT but were affected by instrument problems and not used.

Follow-up observations of PSS J0052+2405 were obtained at the W. M. Keck Observatory Keck I 10 m telescope on 1997 October 4 UT, using the Low Resolution Imaging Spectrometer (LRIS; Oke et al. 1995), in good conditions. A single 1800 s integration was obtained using a 600 lines mm^{-1} grating centered at $\lambda \sim 6000$ Å and covering

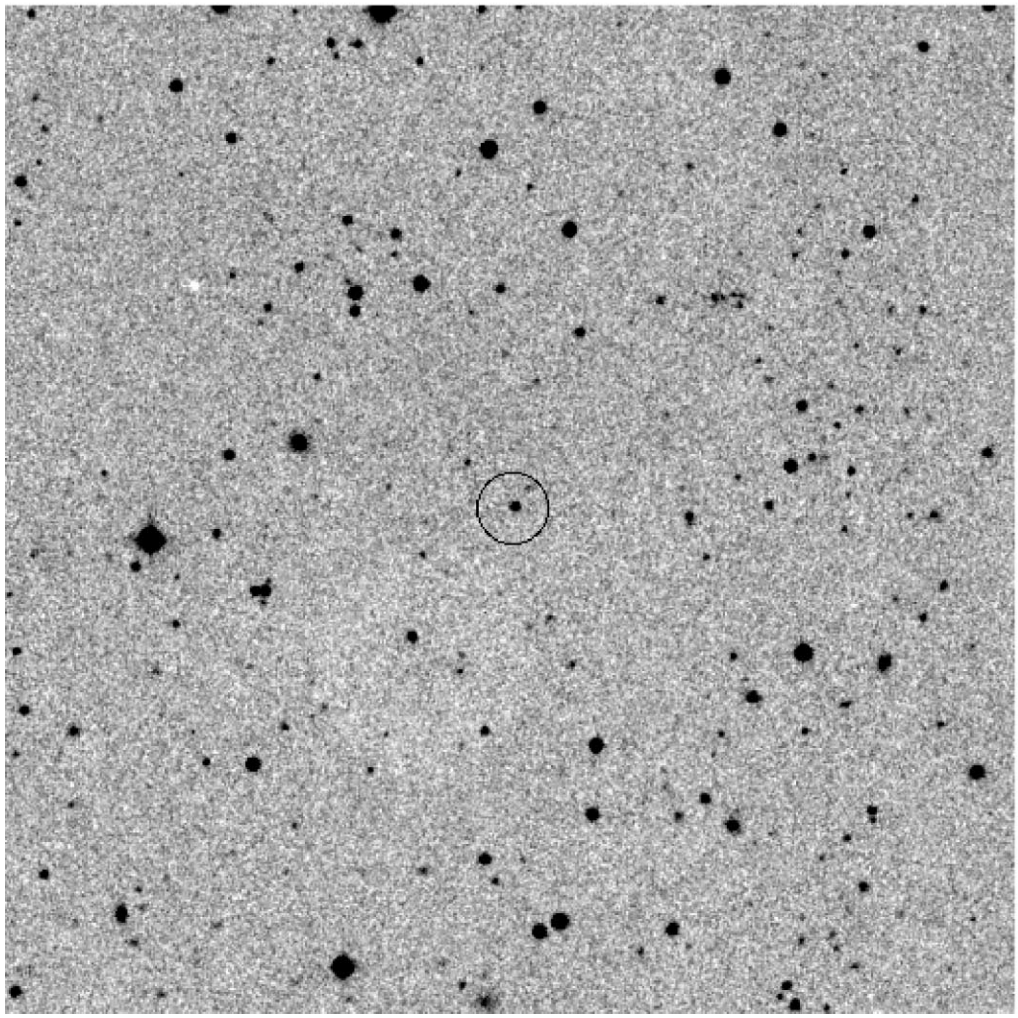

FIG. 2.—A 512 × 512 pixel image (~8.′5 × 8.′5) in the *F* band, centered on PSS 0052+2405, which is circled. In this image, north is up and east is right.

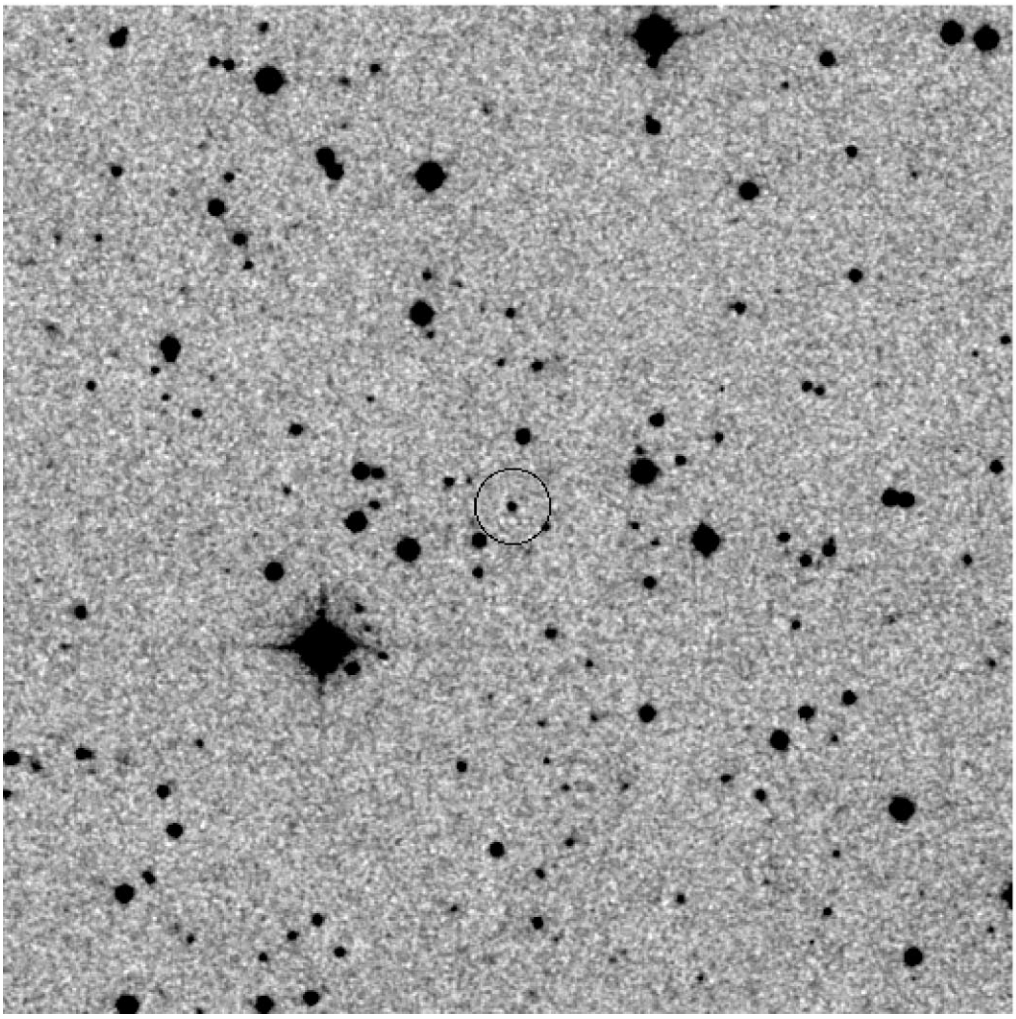

FIG. 3.—Same as Fig. 2, but for PSS 0141+3334

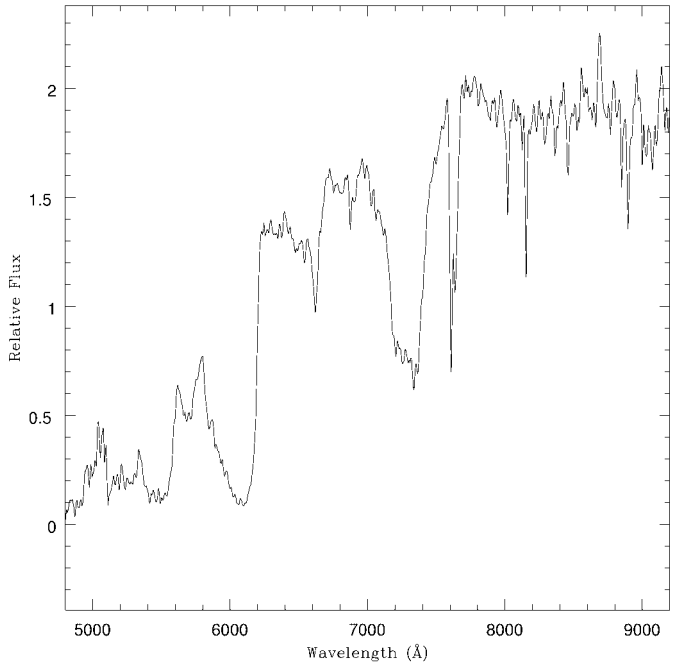

FIG. 4.—Discovery spectrum (f_ν vs. λ) for PSS J0141+3334, obtained using DBSP (Oke & Gunn 1982) on the Hale 200 inch telescope.

a wavelength range of ~4800 to ~7300 Å, with a dispersion of 1.25 Å pixel^{-1} and a FWHM resolution of ~9 Å through a 1.″5 wide slit. These data were superseded by a moderate-resolution spectrum obtained at the Keck II 10 m telescope on 1999 December 30 UT, using the Echellette Spectrograph and Imager (ESI; Sheinis et al. 2002). Exposures of 900 and 1500 s were obtained, in good conditions. The instrument resolution is a constant 11.4 km s^{-1} pixel^{-1} or FWHM ~74 km s^{-1} through the 1.″0 slit, and it covers nearly the entire visible light window from ~3900 to ~11000 Å. This is the discovery spectrum shown in Figure 6 and used in the analysis presented in this paper.

Follow-up observations of PSS J1537+1227 were obtained using LRIS as follows. On 1998 April 2 UT, we obtained two exposures of 600 s, using a 400 lines mm^{-1} grating covering a wavelength range from ~5850 to ~9550 Å, giving a resolution of FWHM ~13 Å through a 1.″5 wide slit. On 1998 April 3 UT, we obtained two exposures of 600 s, using a 300 lines mm^{-1} grating covering a wavelength range from ~3900 to ~9000 Å, giving a resolution of FWHM ~17 Å through a 1.″5 wide slit. On 1999 June 12 UT, we obtained an additional two exposures of 600 s and two of 900 s using the same grating and wavelength coverage, but with a 1″ wide slit, giving a resolution of FWHM ~12 Å. In addition, we also obtained two exposures of

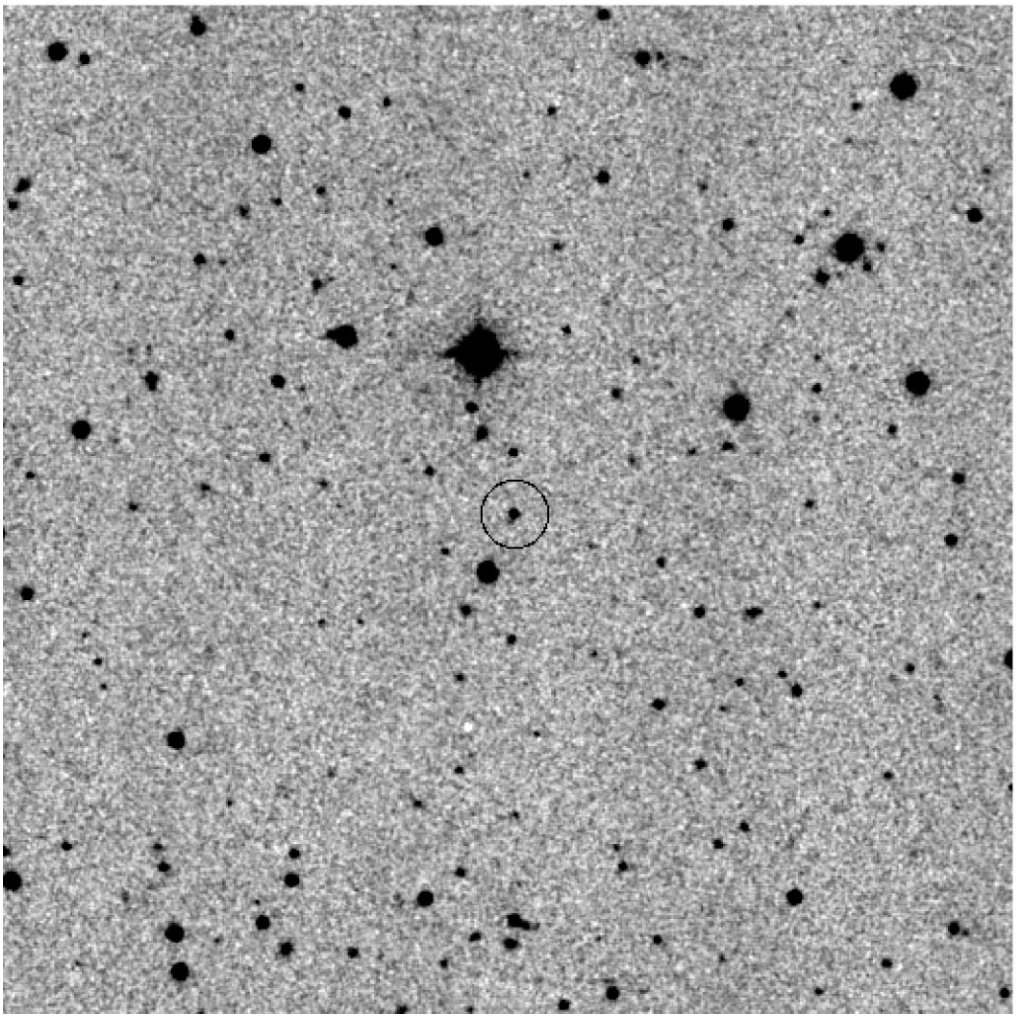

FIG. 5.—Same as Fig. 2, but for PSS 1537+1227

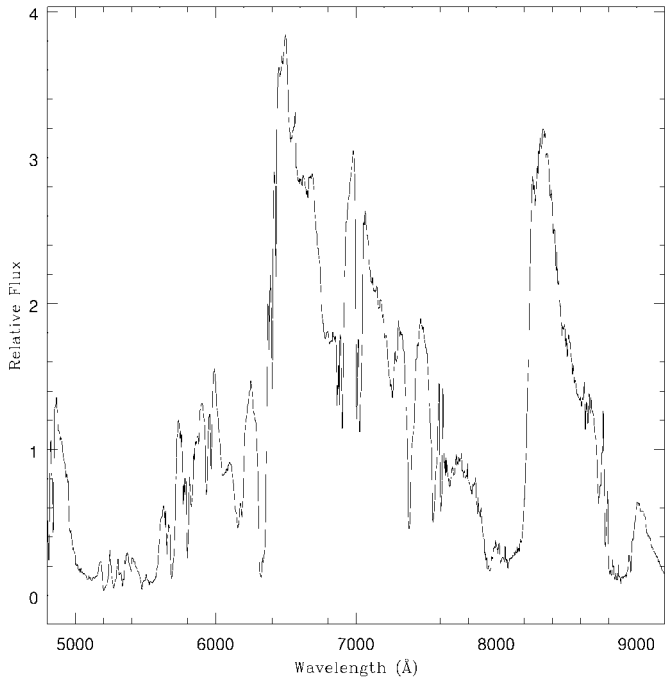

FIG. 6.—Discovery spectrum (f_ν vs. λ) for PSS J0052+2405, obtained using ESI (Sheinis et al. 2002) on the Keck I telescope.

1200 s using a 600 lines mm^{-1} grating covering a wavelength range from ~5900 to ~8450 Å, giving a resolution of FWHM ~6 Å through a 1″ wide slit. The 1998 April data were obtained in photometric conditions, but the 1999 June data were taken through a thin cirrus. All of the LRIS data were reduced and calibrated in a standard manner. This is the discovery spectrum shown in Figure 7 and used in the analysis presented in this paper.

2.2. *Near-Infrared Spectroscopy*

An *H*-band spectrum of PSS J1537+1227 was obtained on UT 1999 August 21 using the facility near-infrared spectrograph NIRSPEC (McLean et al. 1998) on the Keck II telescope. The NIRSPEC detector is an ALADDIN 1024^2 pixel InSb array. The low-resolution mode was used with an 0.″57 wide (4 pixel) slit, giving a spectral resolution of $R \sim 1500$. Two exposures of 600 s were obtained on the source, dithered 14″ along the slit. Two exposures of SAO 101725, an A2 IV star, were also obtained at similar air mass to remove the effects of atmospheric absorption. Dome flats were used to correct for the pixel-to-pixel variations in detector quantum efficiency.

Low-resolution spectra from NIRSPEC are rotated by ~5°, as well as having significant distortions relative to perfect alignment with the rows and columns of the detector.

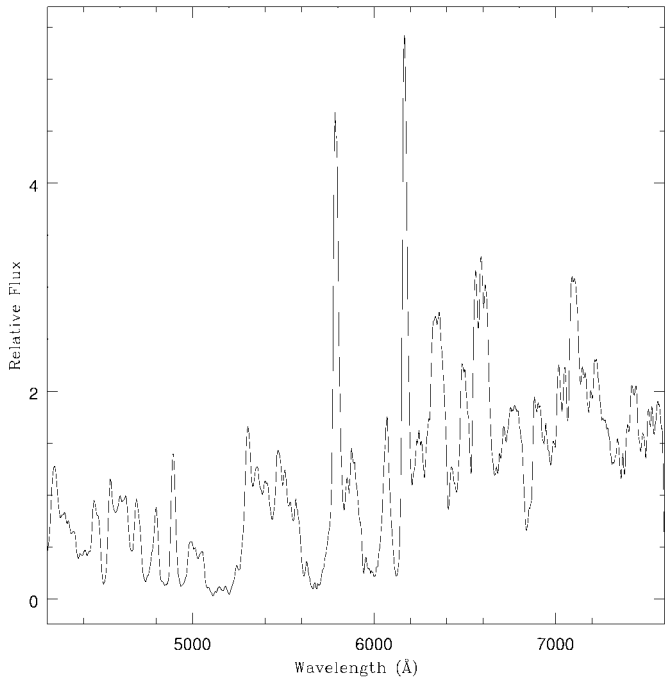

FIG. 7.—Discovery spectrum (f_ν vs. λ) for PSS J1537+1227, obtained using LRIS (Oke et al. 1995) on the Keck I telescope.

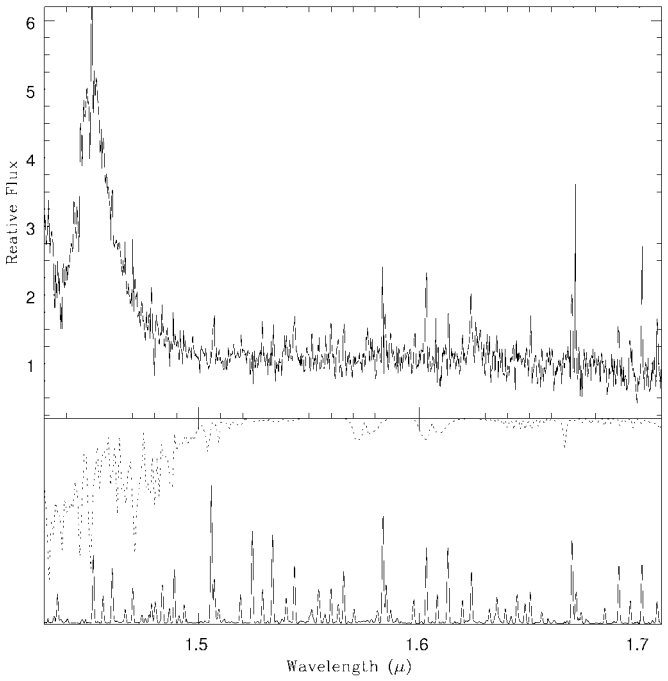

FIG. 8.—Infrared spectrum (relative flux vs. wavelength) for PSS J1537+1227, obtained using NIRSPEC (McLean et al. 1998) on the Keck II telescope. *Top*, the actual spectrum; *bottom*, the sky spectrum (*solid line*) and the relative atmospheric absorption (*dotted line*).

To reduce the data, we first identified and interpolated over the obvious bad pixels and cosmic rays in each frame so they would not be smeared out by further processing. The data were then flat-fielded with a normalized dome flat and the spectra rotated and chopped to cover the area spanned by the 42″ long slit. Each frame was corrected using a distortion map made from the night-sky OH emission lines.

Individual spectra were extracted across an 11 pixel (1.″6) window using variance weighting in the IRAF[9] APEXTRACT package. Wavelength calibration was determined from the night-sky OH emission lines, which show a residual rms scatter of 0.5 Å. The atmospheric extinction was removed by dividing the spectra by the standard star normalized by a 9730 K blackbody spectrum, corresponding to the standard's A2 IV spectral type, covering the same wavelength range. The two spectra of PSS J1537+1227 were then averaged. The final near infrared spectrum of PSS J1537+1227 is shown in Figure 8.

3. PECULIAR BAL QUASARS

In this section, we provide an individual analysis for each of the three peculiar BAL quasars presented in this paper. Identification of the absorption lines (using Moore 1950, 1962) and analysis of the individual spectra follow the techniques outlined in Hall et al. 2002. In particular, for all objects we quote both the traditional "BALnicity index" (BI; Weymann et al. 1991) and the restrictive absorption index (AI; Hall et al. 2002). The AI is designed to include objects with troughs that are relatively narrow or close to the quasar redshift, since detailed studies show that such troughs often share many of the characteristics of BAL troughs.

3.1. *PSS J0052+2405*

PSS J0052+2405 is an FeLoBAL quasar with very broad absorption from many species, presented in Figure 9. We adopt $z = 2.4512 \pm 0.0001$ from narrow Si IV and Al III $\lambda\lambda$1854, 1862 absorption. The long-wavelength end of our spectrum is a trough from Fe II + Mg II; moving toward shorter wavelengths, the spectrum recovers before encountering another Fe II trough near 2400 Å, recovers again near C III] λ1908 before encountering Al III $\lambda\lambda$1854, 1862 absorption, and finally shows a weak recovery at Si IV. C IV is not prominent because of overlying absorption from Fe II multiplets UV42–UV46, similar to SDSS 0437−0045 (Hall et al. 2002).

Many species are detected at the peak absorption redshift of $z = 2.406$, including Si IV, Si II, C IV, Al II, Al III, Ni II, Zn II, Cr II, Mn II, and numerous Fe II multiplets (including UV42–UV43, which are likely responsible for the trough at the expected wavelength of He II λ1640). The highest numbered Fe II multiplets readily identifiable are UV79 and UV80, which arise from terms ~1.7 eV above ground.

Zn II and Cr II are comparably strong at $z = 2.406$ in this object, indicating little dust. What appears to be additional Zn II at slightly lower $z = 2.39$ without accompanying Cr II is in fact residuals from telluric absorption.

There are only two or three possible continuum windows in our spectrum, so it is impossible to say how much this object might be reddened. We do roughly estimate the BI and AI values from the Al II trough using the continuum shown in Figure 9. We measure BI = 1090 km s^{-1} and

[9] IRAF is distributed by the National Optical Astronomy Observatory, which is operated by the Association of Universities for Research in Astronomy, Inc., under cooperative agreement with the National Science Foundation.

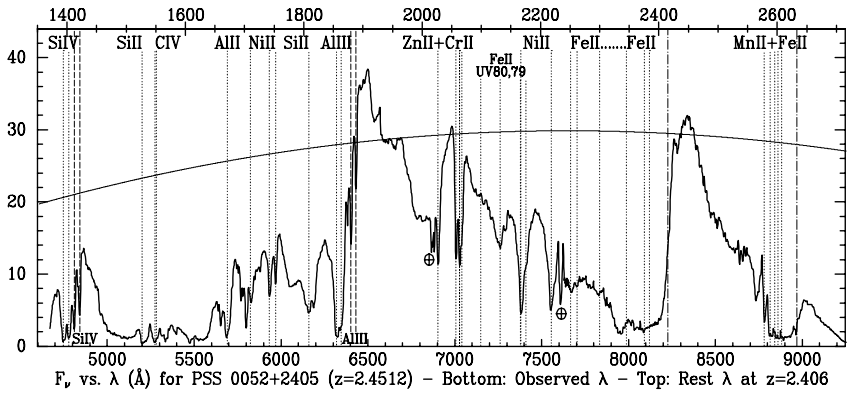

FIG. 9.—Spectrum of the FeLoBAL PSS J0052+2405, with observed wavelengths along the bottom axis and rest-frame wavelengths at the peak absorption redshift of $z = 2.406$ along the top. The vertical scale is F_ν in units of 10^{-1} mJy. Dotted lines indicate absorption at $z = 2.4512$. Dashed lines indicate absorption at $z = 2.406$. Dot-dashed lines show the reddest excited Fe II lines in the complexes around 2400 and 2600 Å. The thin solid line is the continuum fit adopted for calculation of the BI. Telluric absorption is indicated by circled plus signs.

AI = 4240 km s^{-1}. The absorption extends to a velocity of at least 7180 km s^{-1}, beyond which there is confusion with a Si II trough.

3.2. *PSS J0141+3334*

PSS J0141+3334 is a reddened LoBAL quasar at $z = 3.005 \pm 0.005$, as estimated from the red edges of the Si IV, C IV, and Al II absorption troughs, seen in Figure 10. This may be a slight underestimate, since the Al III and possibly the N V troughs may set in at slightly higher redshift. Al II has its peak absorption depth at $z = 2.962$, while the peak depth of Al III is at higher outflow velocity. There appears to be another trough at 1430 Å (assuming $z = 3.005$), but its identification is unclear. An S I identification would be surprising given the lack of absorption from other neutral species that are not shielded from ionization by H I. There is also narrow intervening Fe II absorption in the spectrum at $z = 2.422$ and Mg II absorption at $z = 2.3325$; the latter system may also show weak Fe II absorption.

The steep continuum of PSS J0141+3334 below ~2000 Å rest frame is likely due to dust reddening, because there are no plausible transitions that could blanket the spectrum with absorption shortward but not longward of Al III. The spectrum just longward of C IV at 1550–1600 Å is probably close to the true continuum level, rather than being the bottom of an extended Al II trough.

We adopt the continuum shown in Figure 10. There may be weak broad C IV emission above this continuum, and broad C III] as well, but in general the broad emission in this object appears weak or absorbed. We estimate a SMC extinction law color excess $E(B-V) = 0.30 \pm 0.03$ from comparison of our adopted continuum with the composite SDSS quasar of Vanden Berk et al. (2001). We also measure BI = 10,230 km s^{-1} and AI = 13,800 km s^{-1} from the C IV trough using this continuum and a limiting velocity of 20,410 km s^{-1} to avoid confusion with the 1430 Å trough.

3.3. *PSS J1537+1227*

PSS J1537+1227 is a FeLoBAL with strong narrow Mg II and Fe II emission, presented in Figure 11; a less extreme example is FIRST 0840+3633 (Becker et al. 1997). It has a redshift of $z = 1.212 \pm 0.007$, as determined from the broad Hα line in its *H*-band spectrum, shown in Figure 12. Hα is no doubt blended with [N II], but there is no sign of [S II] or other, weaker lines in the spectral range covered. The rise at the short wavelength end of the *H*-band spectrum is probably not real, since it does not match any known strong line or Fe II blend.

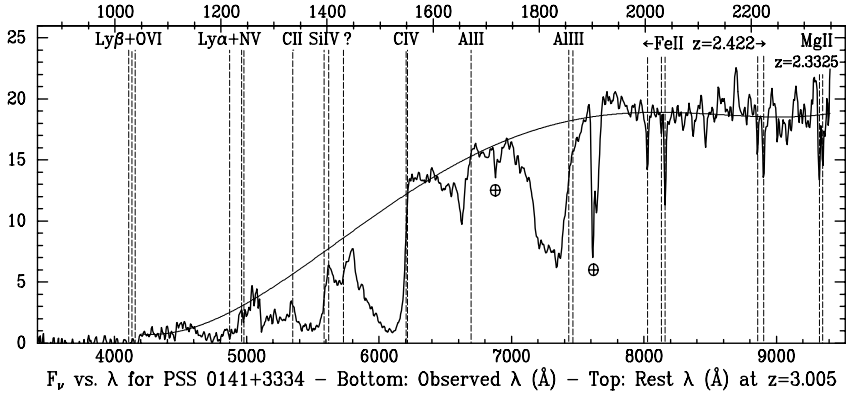

FIG. 10.—Spectrum of the LoBAL PSS J0141+3334, plotted in the same manner as Fig. 9. Dashed lines are labeled with the transition and redshift of the indicated absorption; transitions without a redshift label are plotted at the systemic redshift of $z = 3.005$.

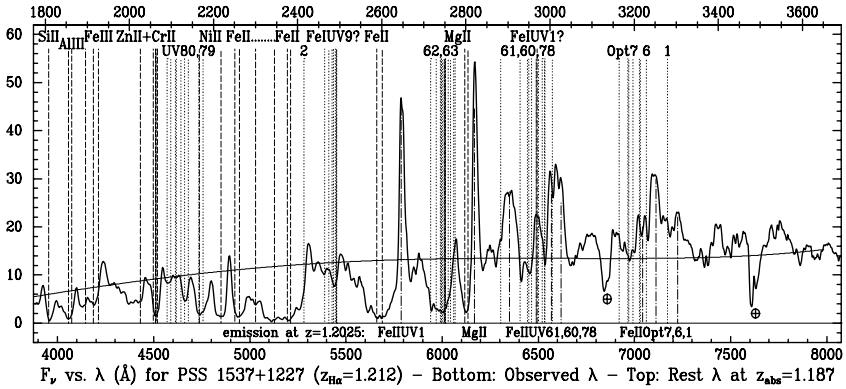

FIG. 11.—Spectrum of the FeLoBAL PSS J1537+1227, plotted in the same manner as Fig. 9. Transitions in absorption are labeled across the top of the plot. Dashed lines show confirmed transitions in absorption at $z = 1.187$; dotted lines show excited-state Fe II transitions at that z. Fe II ultraviolet (UV) and optical (Opt) multiplets are numbered in the second line of labels across the top. Transitions in emission are labeled across the bottom of the plot. Dot-dashed lines show narrow emission at $z = 1.2025$ from Mg II and various Fe II multiplets.

PSS J1537+1227 has Mg II and Fe II UV1 emission (*dot-dashed lines*) that is much narrower than the Hα emission. The redshift from Mg II is $z = 1.2025 \pm 0.0005$, which is a blueshift of 1290 ± 950 km s^{-1} from the Hα redshift. The absorption troughs appear deepest at $z = 1.187$, a further blueshift of 2120 km s^{-1}. Blueward of Mg II, the spectrum includes absorption from Si II, Al III, Fe III UV34 (near 1910 Å), Cr II + Zn II, Ni II, and numerous Fe II multiplets (dotted lines) up to at least UV79 and UV80 ($\sim$1.7 eV above ground; cf. PSS J0052+2405).

Absorption from He I λ3188 and He I λ2946 may also be present, and possibly weak Mg I λ2852. These features are useful diagnostics of physical conditions in the BAL gas, but a higher resolution spectrum is needed to sort out which of them are in fact present.

It is difficult to know where to place the continuum, since the spectrum is a complex blend of Fe II emission and absorption even longward of Mg II. There is certainly some Fe II UV60, UV61, and UV78 absorption at 2860–3000 Å rest frame, since absorption from multiplets up to UV80 and Opt7 are identifiable elsewhere in the spectrum.

In Figure 11, we use dotted lines to show the wavelengths of these strong absorption lines of excited Fe II and dot-dashed lines to show emission from multiplets UV1, UV60, UV61, and UV78 and Opt1, Opt6, and Opt7.

The good agreement of the dot-dashed lines with the emission peaks and the dashed lines with the absorption shows that the spectrum can be understood as emission at $z = 1.2025$ coupled with absorption that is strongest at $z = 1.187$. We note that the relative strengths of the UV1, UV61, UV60+UV78, and Opt7 Fe II emission peaks may be in better agreement with theoretical models than the spectrum of QSO 2226−3905 studied in de Kool et al. (2002). Contrary to their suggestion of a problem with the models, it may just be that the Fe II emission line regions span a wider range of physical conditions than considered in their modeling. However, it is also true that the relative strengths of the Fe II lines in PSS J1537+1227 are affected by absorption. In particular, the UV2 and UV62,UV63 peaks are much weaker here than in theoretical models. More detailed modeling based on higher resolution spectra is needed to determine whether this is a problem with the theory or whether it can be explained by overlying absorption.

There is in fact at least a weak absorption trough in this object that hints that the absorption may be even more complicated than it appears. The $\sim$2480 Å trough might be explained as Fe I UV9. However, there is no corresponding trough of Fe I UV1 at 2970 Å, which should be at least as strong. In fact, there is a local maximum at the expected wavelength of Fe I UV1. Fe II emission could conceivably

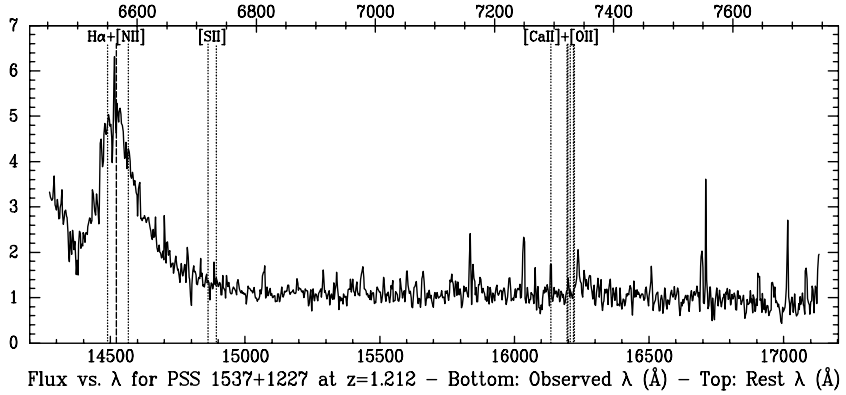

FIG. 12.—Infrared (*H*-band) spectrum of the FeLoBAL PSS J1537+1227. Dashed lines show emission at the adopted systemic $z = 1.212$. The vertical scale is relative flux in arbitrary units.

hide a Fe I UV1 trough, but that would require that the true peaks of the emission lines be considerably higher than observed. Nonetheless, we cannot rule out the presence of Fe I without a higher resolution spectrum. Such spectroscopy would constrain the physical parameters of the BAL outflow even if no Fe I is present (e.g., de Kool et al. 2002), but would do so even more tightly if it is. This is because Fe I has an ionization potential less than that of H I and so is only found in gas with a low-ionization parameter, which makes it a very useful diagnostic.

For now, since Fe I is rarely seen in BAL outflows, we conservatively assume that only Fe II is present in this object, which allows us to make an educated guess about the continuum level. There are no strong Fe II transitions immediately redward of 2800 and 3000 Å, so we adopt those as continuum windows, along with regions near 3350 and 3600 Å, which are also free of strong Fe II transitions from terms $\lesssim 4$ eV above ground.

Adopting the continuum shown in Figure 11, we find from the Mg II trough that AI = 1780 km s^{-1} but that the BI is only marginally nonzero (3 km s^{-1}), since the Mg II absorption trough only extends $\sim$5035 km s^{-1} shortward of the systemic redshift.

4. DISCUSSION

The three peculiar BAL quasars presented in this paper were selected from DPOSS (Djorgovski et al. 2001) due to their unusual locations within the $g-r$ versus $r-i$ color space. While large, multiband photometric surveys, such as DPOSS, provide great opportunities for improving the statistical quantification of different astrophysical source classes, the challenge of finding novel sources is equivalent to finding needles in a haystack. When the number of detected sources in surveys of this type exceed 100 million, even well-intentioned color selections can fail to uncover possible interesting sources, and the resulting selection effects can be difficult—if not impossible—to completely characterize.

To demonstrate this difficulty, we examined the locus traced by these quasars in the target color space as their observed emission redshift was synthetically shifted ($\Delta z = \pm 0.1$). This process involved shifting each individual spectrum, both blueward and redward, and convolving the resulting spectrum with the g, r, and i digital filter curves, obtained from the Palomar Observatory Web site. In several cases, the shifted spectrum did not completely cover the same wavelength range as one of the two end filters (i.e., g or i). To account for this, the spectrum was extended across the necessary wavelength range by extrapolating the last flux value. In no case did this small approximation make any significant contribution to the resulting flux measurements (which is obvious since the filters fall sharply at their edges).

The results are shown in Figure 13, where the three quasars presented in this paper are shown along with random sources from DPOSS and other BAL quasars drawn from the Junkkarinen, Hewitt, & Burbidge (1991) compilation, which are displayed using their colors as measured by DPOSS. The BAL quasars, including the peculiar BAL quasars presented herein, are differentiated based on their redshift: $1 \leq z < 2$ (*triangles*), $2 \leq z < 3$ (*squares*), and $z > 3$ (*circles*). The arrows on the three sources presented in this paper show the new location of these quasars after changing their redshift by ± 0.1 (lower arrows result from shifting the spectrum to the red and the upper arrows result from shifting the spectrum to the blue). While not shown, we note that for comparison unusual BAL quasars found within SDSS data (Hall et al. 2001) are considerably redder than normal quasars in $g-r$ and slightly redder in $r-i$.

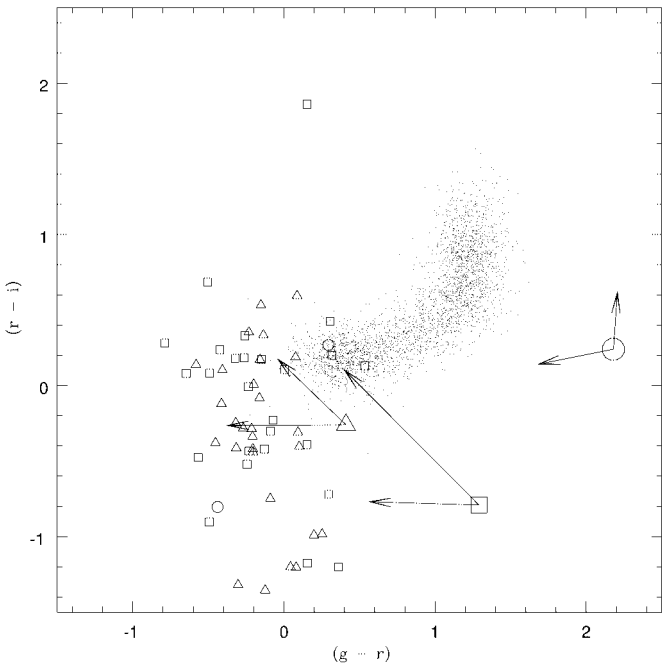

FIG. 13.—Same color space and data as shown in Fig. 1, with the addition of other BAL quasars drawn from the Junkkarinen et al. (1991) compilation, which are displayed using their colors as measured by DPOSS. The three large symbols indicate the three quasars presented in this paper. The BAL quasars, including the peculiar BAL quasars presented herein, are differentiated based on their redshift: $1 \leq z < 2$ (*triangles*), $2 \leq z < 3$ (*squares*), and $z > 3$ (*circles*). The arrows on the three sources presented in this paper show the new location of these quasars after changing their redshift by ± 0.1 (lower arrows result from shifting the spectrum to the red and the upper arrows result from shifting the spectrum to the blue).

While this figure demonstrates several things, the most important is the sensitivity of the location of these sources within color space to their actual redshift. Two of these sources, PSS J0052+2405 and PSS J0141+3334, actually disappear into the stellar locus when their spectra are shifted blueward. This raises the possibility of additional peculiar sources lurking among the stars. In order to find them, data from multiple surveys (preferably covering different wavelength regions) will need to be federated. This results in a data set that presents intense computational challenges due to the higher dimensional parameter space through which the algorithms must search. Through collaborations with computer scientists and statisticians, however, new algorithms and approaches (e.g., Connolly et al. 2000) are being developed that provide possible solutions to this technical hurdle.

An additional point of interest is the lack of differentiation between BAL quasars at different redshifts in this two-dimensional parameter space. This degeneracy could potentially be lifted with additional imaging data and could prove to be an interesting application area for data mining algorithms. This is an area where medium-band spectrophotometric surveys (e.g., Combo 17)[10] or multiwavelength data

[10] See http://www.mpia-hd.mpg.de/COMBO/combo_index.html.

federation projects (e.g., Brunner 2001) may provide fruitful input data sets.

In order to roughly estimate the rarity of these objects, we consider the following. These quasars have been found in the course of a search for high-z and type 2 QSOs, which covered the area of approximately 10^4 deg^2. At the brightness level of these sources, the spectroscopic follow-up is nearly complete, in the corresponding region of the *gri* color space. Thus, the implied surface density of these objects, down to this magnitude level and within the region of the color space searched, is roughly $\sim 3 \times 10^{-4}$ deg^{-2}. While we do not have any reliable way of estimating how many more such objects exist outside our region of the color space, it is likely that the total (color-independent) surface density would be a factor of a few higher. While all three sources have $r < 19$ mag, our search was nearly complete down to this flux level. The cumulative surface density of all QSOs down to such magnitude levels is approximately a few times 10 deg^{-2} (e.g., Schneider et al. 2002). Thus, we conservatively conclude that $\sim 10^{-4}$ of all QSOs belong to this peculiar subclass.

To conclude, in this paper we have presented three peculiar BAL quasars from the Digitized Palomar Observatory Sky Survey: PSS J0052+2405, PSS J0141+3334, and PSS J1537+1227.

PSS J0052+2405 is an FeLoBAL quasar at a redshift $z = 2.4512 \pm 0.0001$ with many species detected at the peak absorption redshift of $z = 2.406$, including Si IV, Si II, C IV, Al II, Al III, Ni II, Zn II, Cr II, Mn II, and numerous Fe II multiplets.

PSS J0141+3334 is a LoBAL quasar at $z = 3.005 \pm 0.005$ with several species seen in absorption, including Si IV, C IV, and Al II. There is also narrow intervening absorption at lower redshifts from Fe II and Mg II.

PSS J1537+1227 is a FeLoBAL quasar at $z = 1.212 \pm 0.007$ and is an excellent target for high-resolution spectroscopy, since it has very narrow absorption lines and may show absorption from numerous useful diagnostic transitions.

The ability of large velocity width, high covering factor absorption to blanket large regions of the spectrum in BAL quasars raises the possibility that quasar surveys based on blue colors have systematically missed such objects. The true ranges of these and other BAL properties remains to be characterized, most notably upper limits for the column densities of the various ions which can be found in LoBAL outflows (Hall et al. 2003).

R. J. B. acknowledges partial support from NASA ADP (NAG 5-10885), NASA AISRP (NAG 5-12000), and the Fullam Award. P. B. H. acknowledges financial support from Chilean grant FONDECYT/1010981 and a Fundación Andes grant. The authors gratefully acknowledge those of Hawaiian ancestry on whose sacred mountain we are privileged to be guests. Without their generous hospitality, none of the observations presented would have been possible. The processing of DPOSS and the production of the Palomar-Norris Sky Catalog (PNSC) on which this work was based was supported by generous grants from the Norris Foundation and other private donors. Some of the software development was supported by the NASA AISRP program. We also thank the staff of Palomar Observatory for their expert assistance in the course of many observing runs. Finally, we acknowledge the efforts of the POSS-II team and the plate scanning team at STScI.

REFERENCES

Becker, R. H., Gregg, M. D., Hook, I. M., McMahon, R. G., White, R. L., & Helfand, D. J. 1997, ApJ, 479, L93
Boyle, B. J., Croom, S. M., Smith, R. J., Shanks, T., Miller, L., & Loaring, N. 1999, in Looking Deep in the Southern Sky, ed F. Morganti & W. J. Couch (Berlin: Springer), 16
Brunner, R. J. 2001, Proc. SPIE, 4477, 1
Connolly, A. J., Genovese, C., Moore, A. W., Nichol, R. C., Schneider, J., & Wasserman, L. 2000, AJ, submitted
de Kool, M., Becker, R. H., Gregg, M. D., White, R. L., & Arav, N. 2002, ApJ, 567, 58
Djorgovski, S. G., et al. 2001, in Mining the Sky, ed. A. J. Banday, S. Zaroubi, & M. Bartlemann (Berlin: Springer), 305
Gal, R. R., de Carvalho, R. R., Lopes P. A., Djorgovski, S. G., Brunner, R. J., Mahabal, A. A., & Odewahn, S. C. 2003, AJ, 125, 2064
Hall, P. B., et al. 2002, ApJS, 141, 267
———. 2001, in ASP Conf. Ser. 255, Mass Outflow in Active Galactic Nuclei: New Perspectives, ed. D. M. Crenshaw, S. B. Kraemer, & I. M. George (San Francisco: ASP), 161
Hall, P. B., Hutsemékers, D., Anderson, S. F., Brinkmann, J., Fan, X., Schneider, D. P., & York, D. G. 2003, ApJ, submitted (astro-ph/0301480)
Junkkarinen, V., Hewitt, A., & Burbidge, G. 1991, ApJS, 77, 203
Lasker, B. M., Doggett, J., McLean, B., Sturch, C., Djorgovski, S., de Carvalho, R. R., & Reid, I. N. 1996, in ASP Conf. Ser. 101, Astronomical Data Analysis Software and Systems V, ed. G. H. Jacoby & J. Barnes (San Francisco: ASP), 88
Mahabal, A. A., Djorgovski, S. G., Gal, R. R., Odewahn, S. C., de Carvalho, R. R., & Brunner, R. J. 2003, in preparation
McLean, I. S., et al. 1998, Proc. SPIE, 3354, 566
Moore, C. E. 1950, An Ultraviolet Multiplet Table, Sections 1–2 (NBS Circ. 488) Washington: US Gov. Printing Off.)
———. 1962, An Ultraviolet Multiplet Table, Section 4 (NBS Circ. 488) (Washington: US Gov. Printing Off.)
Odewahn, S. C., Gal, R. R., Djorgovski, S. G., Mahabal, A. A., & Stalder, B. 2003, AJ, submitted
Oke, J. B., et al. 1995, PASP, 107, 375
Oke, J. B., & Gunn, J. E. 1982, PASP, 94, 586
———. 1983, ApJ, 266, 713
Reid, I. N., et al. 1991, PASP, 103, 661
Sandage, A. 1965, ApJ, 141, 1560
Schlegel, D. J., Finkbeiner, D. P., & Davis, M. 1998, ApJ, 500, 525
Schneider, D. P., et al. 2002, AJ, 123, 567
Scoville, N., & Norman, C. 1995, ApJ, 451, 510
Sheinis, A., Bolte, M., Epps, H., Kibrick, R., Miller, J., Radovan, M., Bigelow, B., & Sutin, B. 2002, PASP, 114, 851
Small, T. A., & Blandford, R. D. 1992, MNRAS, 259, 725
Vanden Berk, D. E., et al. 2001, AJ, 122, 549
Weir, N., Fayyad, U. M., Djorgovski, S. G., & Roden, J. 1995, PASP, 107, 1243
Weymann, R. J. 1995, QSO Absorption Lines, ed. G. Meylan (New York: Springer), 213
Weymann, R. J., Morris, S. L., Foltz, C. B., & Hewett, P. C. 1991, ApJ, 373, 23
York, D. G., et al. 2000, AJ, 120, 1579